Universal scaling in a strongly interacting Rydberg gas

Robert Löw,[1,*] Hendrik Weimer,[2] Ulrich Krohn,[3] Rolf Heidemann,[1] Vera Bendkowsky,[1] Björn Butscher,[1] Hans Peter Büchler,[2] and Tilman Pfau[1,†]

[1]*5. Physikalisches Institut, Universität Stuttgart, Pfaffenwaldring 57, 70550 Stuttgart, Germany*

[2]*Institut für Theoretische Physik III, Universität Stuttgart, 70550 Stuttgart, Germany*

[3]*Department of Physics, Durham University, Durham DH1 3LE, United Kingdom*

(Received 25 February 2009; revised manuscript received 14 August 2009; published 29 September 2009)

We study a gas of ultracold atoms resonantly driven into a strongly interacting Rydberg state. The long-distance behavior of the spatially frozen effective pseudospin system is determined by a set of dimensionless parameters, and we find that the experimental data exhibit algebraic scaling laws for the excitation dynamics and the saturation of Rydberg excitation. Mean-field calculations as well as numerical simulations provide an excellent agreement with the experimental finding and are evidence for universality in a strongly interacting frozen Rydberg gas.

DOI: 10.1103/PhysRevA.80.033422 PACS number(s): 32.80.Ee, 64.70.Tg, 67.85.−d

I. INTRODUCTION

The concept of universality appears in many different fields of physics [1], biology [2], economics [3], and various other systems. It allows to describe the behavior of a system without actually knowing all the microscopic details of its state. A particular class of universal scaling behavior can be found close to second-order phase transitions. The characterization of the corresponding critical points in terms of universality classes [4] has become crucial for the understanding of classical as well as quantum phase transitions. Quantum degenerate gases can serve as a well-controlled model system for the exploration of universal scaling behavior and quantum phase transitions [5] in strongly interacting cold atomic systems. Here, we show that the experimental data support the appearance of universal scaling in ultracold Rydberg gases, which is in agreement with the recently predicted existence of a quantum critical point [6].

The key ingredients of the described experiments are the combination of a Rydberg gas in the "frozen" regime [7] with strong interactions among the Rydberg atoms [8] and the ability to coherently drive the system [9] as a pseudospin. There exists a variety of interaction mechanisms among Rydberg atoms giving rise to blockade phenomena, which are intensively studied [8,10,11] experimentally. Recently, several groups also focused on the coherent properties of frozen Rydberg gases in the regime of weak [12–14], as well as strong interactions [9,15–18]. This unique combination of strong interactions with long coherence times led to various proposals for quantum information processing using Rydberg atoms [19–22].

In this work, we apply the theoretical framework of a quantum critical behavior in strongly interacting Rydberg gases [6] to experimental data [see Fig. 1(a)], which has been previously analyzed with respect to coherent and collective excitation of Rydberg atoms in the strong blockade regime [8]. The relevant parameters of the experiment are the density of particles n, the coupling strength of the driving laser field Ω [see Fig. 1(b)], its detuning from resonance δ_L, and the interaction strength among the Rydberg states determined in our case by the van der Waals constant C_6. On resonance ($\delta_L=0$), these parameters can be merged into a single dimensionless parameter $\alpha=\hbar\Omega/C_6n^2$. We find that all experimental data taken from [8] collapse to a simple power law as a function of this parameter α [see Fig. 1(c)], which is in

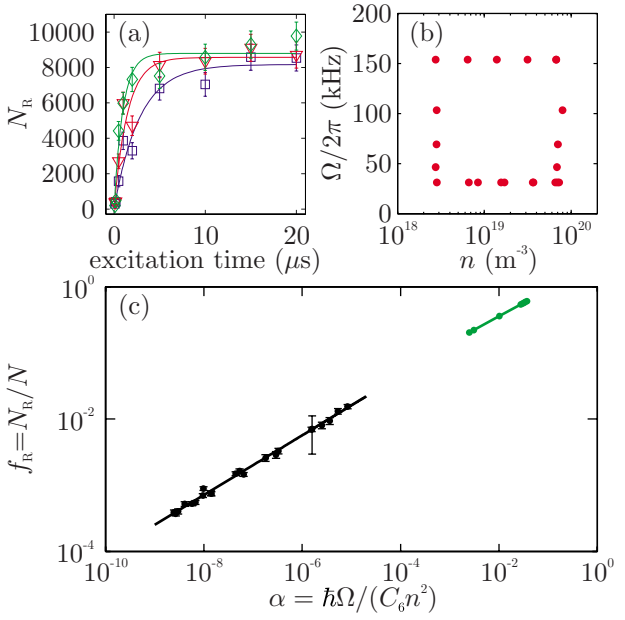

FIG. 1. (Color online) Universal scaling of the Rydberg fraction in the saturated excitation regime (a). The saturated Rydberg excitation is obtained with a laser coupling strength of $\Omega=2\pi\times154$ kHz in dense ultracold atomic clouds with densities $n=[3.2\times10^{19}(\diamond),6.6\times10^{18}(\triangledown),2.8\times10^{18}(\square)]$ m^{-3} [8]. (b) Scanned parameter space for the individual excitation curves depicted in the $n-\Omega$ plane. (c) Saturated Rydberg fraction f_R as a function of the dimensionless parameter $\alpha=\hbar\Omega/C_6n^2$ for a three-dimensional configuration (■) and numerical simulations (●). The experimental and numerical data are fitted (solid lines) to power laws of the form $f_R\sim\alpha^{1/\delta}$ from which the critical exponents $1/\delta=0.45\pm0.01$ (expt.) and $1/\delta=0.404$ (num.) are extracted.

*r.loew@physik.uni-stuttgart.de

†t.pfau@physik.uni-stuttgart.de

agreement with the predicted universal scaling behavior. This implies that the interpretation in terms of a continuous quantum phase transition [6] is supported by experimental data and thus provides a firmer theoretical foundation compared to previous scaling models [8]. While the scaling models essentially depend on two parameters (Rabi frequency and ground-state density), there is only one single parameter in the universal scaling function, which is the length scale diverging at the critical point. We also show that these scaling models can be rigorously derived from the mean-field approach given in [6].

II. UNIVERSAL SCALING THEORY

Textbooks on statistical mechanics [1] often introduce universal scaling as a critical phenomenon, which can be found near the critical point of a second-order phase transition. When approaching the critical point, the system becomes scale invariant. This means that microscopic details of the system become irrelevant, and the macroscopic behavior is dominated by its long-range physics associated with a diverging length scale ξ. Mathematically, a function $f(s)$ is called scale invariant, if $f(\lambda s)=cf(s)$. Using a series expansion, one can see that solutions to this equation are given by power laws of the form $f(s)\propto s^{\nu}$. Hence, near the critical point all observables can be described by power laws of the diverging scale ξ. Since the critical properties are dominated by long-range physics, many different systems show the same critical behavior. This leads to the classification of critical exponents in terms of universality classes, which are determined by the spatial dimension, the symmetries of the Hamiltonian, and the long-range behavior of the interactions.

Phase transitions occur when the free energy of a system shows nonanalytic behavior. In classical systems, this is always related to a change in temperature. However, in quantum systems at $T=0$, there is another possibility: the ground-state energy can become nonanalytic in the case of an avoided crossing with vanishing gap or an actual level crossing [23]. Analogously to their classical counterparts, one can classify quantum phase transitions into first-, second-, and infinite-order transitions.

A. Universal scaling in a ferromagnet

The most prominent example of a second-order phase transition is a ferromagnet close to the Curie temperature T_C. For $T>T_C$, the system is completely demagnetized and rotationally invariant. Lowering the temperature below T_C, the system enters the ferromagentic phase characterized by a finite magnetization M, which breaks the rotational symmetry. The appearance of the magnetization can be described in terms of an order parameter. Above T_C, the magnetization M is simply zero and exhibits a linear magnetization in the presence of an external magnetic field H. The equation of state close to the critical point at T_c is shown in Fig. 2(a) in terms of the reduced temperature $t=1-T/T_C$ and the external magnetic field H. Then the system is described in terms of universal scaling laws of the form $M\sim t^{\beta}$ for $H=0$ and $M\sim H^{1/\delta}$ for $t=0$, indicated by the curves ⓐ and ⓑ, while the diverging length satisfies $\xi\sim 1/t^{\nu}$.

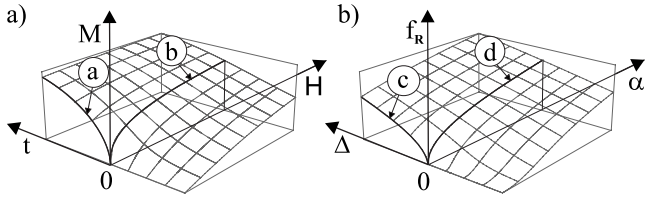

FIG. 2. Equation of state of a ferromagnet in comparison to a strongly interacting Rydberg gas (a) magnetization M of a classical ferromagnetic Ising model: the system exhibits a critical point at $t=1-T/T_c=0$ and $H=0$. The magnetization M is given by a power laws ⓐ $M\sim t^{\beta}$ and ⓑ $M\sim H^{1/\delta}$. The exponents have been calculated with the Ising model to be $\beta=0.31$ (measured: 0.32–0.39) and $\delta=5$ (measured: 4–5) [1]. (b) Excited-state fraction f_R of a strongly interacting Rydberg gas. The universal scaling laws are given by power laws of the rescaled detuning Δ of the driving field ⓒ $f_R(\alpha=0)\sim\Delta^{\beta}$ and the rescaled coupling strength α as depicted by ⓓ $f_R(\Delta=0)\sim\alpha^{1/\delta}$. Within the mean-field theory, the plotted parameter f_R is given for a three-dimensional cloud with van der Waals interaction by $\alpha=f_R^{\delta}|1-\Delta/f_R^{1/\beta}|$ with $\delta=5/2$ and $\beta=1/2$.

B. Universal scaling in a strongly interacting Rydberg gas

Now we want to draw the analogy of the magnet close to the Curie point to a strongly interacting Rydberg gas driven by a laser field. The frozen atomic gas is assumed to consist of an ensemble of spatially fixed pseudospins with two electronic states, one being the ground state and the other a highly excited Rydberg state. The coupling Ω between the two states is achieved by a monochromatic light field with a detuning δ_L with respect to the energy splitting of the two states. The Rydberg states interact strongly with a general interaction potential C_p/r^p, which in the present experimental situation is dominated by the van der Waals interaction with $p=6$. The corresponding N-particle Hamiltonian then reads as

$$H=-\frac{\hbar\delta_L}{2}\sum_i \sigma_z^{(i)}+\frac{\hbar\Omega}{2}\sum_i \sigma_x^{(i)}+C_p\sum_{j<i}\frac{P_{ee}^{(i)}P_{ee}^{(j)}}{|\mathbf{r}_i-\mathbf{r}_j|^p}, \quad (1)$$

where the $\sigma_{x,y,z}^{(i)}$ are Pauli matrices, $\mathbf{r}_i$ is the position of the atom i, and $P_{ee}^{(i)}=(1+\sigma_z^{(i)})/2$ is the projector on the excited Rydberg state. It has been recently shown [6] that this Hamiltonian features a quantum critical point at $\Omega=\delta=0$ for $p>d$, where d is the dimensionality of the system. In contrast to the above classical example, the critical point appears even at zero temperature by varying the detuning δ_L. Consequently, the role of the reduced temperature t is now taken by the dimensionless detuning $\Delta=\hbar\delta_L/E_c$ with the characteristic energy $E_c=C_p n^{p/d}$. For $\Delta<0$, all atoms remain in the ground state for $\Omega\to 0$, while for $\Delta>0$ a finite number N_R of atoms are excited into the Rydberg state. The fraction of excited Rydberg atoms $f_R=N_R/N$ then plays the analog role of the magnetization M in the example of a ferromagnetic phase transition discussed above. In analogy, we can draw the fraction of excited Rydberg atoms f_R close to the critical point as a function of the detuning Δ and the parameter $\alpha=\hbar\Omega/E_c$ [see Fig. 2(b)]. Note that the continuous behavior of f_R at the critical point is a special property of the long-distance

behavior of the interaction potential. The coherence length ξ is determined by the characteristic length scale of the correlation function $\langle (P_{ee}^{(i)}-f_R)(P_{ee}^{(j)}-f_R)\rangle$, which gives rise to a diverging length scale close to the critical point. This quantity corresponds to the blockade radius in the system, i.e., the radius around a Rydberg atom, up to which an additional Rydberg excitation is strongly suppressed.

It remains to identify the critical exponents β and $1/\delta$ for the universal scaling of the observable parameter $f_R \sim \Delta^\beta$ and $f_R \sim \alpha^{1/\delta}$. For $\alpha=0$, the Hamiltonian (1) is classical and by minimizing its energy one obtains $\beta=d/p$. The correlation length ξ is determined by the averaged spacing between the Rydberg atoms via $\xi \sim a/f_R^{1/d}$ (here, $a^{-1}=\sqrt[d]{n}$ denotes the averaged interparticle distance of a d-dimensional system). To obtain a value for $1/\delta$, it is useful to take a closer look at the excitation dynamics of a strongly interacting Rydberg system ($\alpha \ll 1$) driven at resonance ($\Delta=0$), which also complies with the experimental situation [8]. When α approaches zero, the system enters the strongly blocked regime with $f_R \ll 1$. Within the blockade radius ξ, only one excitation is shared over a large number of atoms $N_b \sim n\xi^d$ resulting in a collective state $|\psi_e\rangle = \frac{1}{\sqrt{N_b}}\Sigma_{i=1}^{N_b}|g_1,g_2,g_3,\ldots,e_i,\ldots,g_{N_b}\rangle$, which shows an accelerated temporal evolution with a collective Rabi frequency $\sqrt{N_b}\Omega$ [8,16,24]. In this so-called superatom model, the blockade radius can be evaluated by equating the interaction energy with the collective coupling strength as $C_p/\xi^p=\sqrt{N_b}\Omega$. Note that ξ diverges for $\alpha \to 0$. This procedure determines $1/\delta$ to be $1/\delta=2d/(2p+d)$ and the case for $d=3$ and $p=6$ is carried out in some more detail in [25]. The same result for $1/\delta$ is obtained using standard the mean-field theory [6]. In addition, the mean-field solution leads to a description of the full behavior of f_R in terms of a general scaling function

$$f_R = \alpha^{2d/(2p+d)}\chi\left(\frac{\Delta}{\alpha^{2p/(2p+d)}}\right). \tag{2}$$

This is the inverse of the exact mean-field result $\alpha=f_R^\delta|1-\Delta/f_R^{1/\beta}|$ shown in Fig. 2(b). As the system turns classical in the limit $\alpha \to 0$, the behavior of the unknown function $\chi(y)$ in the limit $y \to \pm\infty$ can exactly be determined to be $\chi(y) \sim y^{d/p}$ and $\chi(y)=1/y^2$, respectively. It is important to note that the mean-field result for δ is the only consistent scaling exponent with these limits. This indicates that the classical behavior of the system at $\alpha=0$ fixes the exponent δ to its mean-field value even for low dimensions. In contrast to a classical critical point, for a quantum critical point, the dynamical behavior is coupled to the static properties via the dynamical critical exponent z, i.e., $\tau \sim \xi^z$, where τ describes the characteristic time scale close to the critical point. Here, we find the dynamical critical exponent to be $z=p$, which implies that the relaxation is domitated by the frequency $\sqrt{N_b}\Omega$ in agreement with the above superatom picture.

III. EXPERIMENT

A. Universal scaling in an inhomogeneous sample

In the actual experiment, the atoms are well described as a thermal gas trapped by a harmonic potential. Then, the three-dimensional density distribution of the N ground-state atoms has a Gaussian shape with radii given by the standard deviations $\sigma_{x,y,z}=\sqrt{k_BT/2m\omega_{x,y,z}}$, which are determind by the trapping frequencies $\omega_{x,y,z}$, the mass m, the temperature T of the cloud, and Boltzmann's constant k_B

$$n(\mathbf{r}) = \frac{N}{(2\pi)^{3/2}\sigma_x\sigma_y\sigma_z}\exp\left(-\frac{x^2}{2\sigma_x^2}-\frac{y^2}{2\sigma_y^2}-\frac{z^2}{2\sigma_z^2}\right). \tag{3}$$

Note that the temperature T associated with the kinetic energy of the atoms is decoupled from the dynamics of the Rydberg excitations in the frozen Rydberg gas. Within the local-density approximation, we can describe the properties of the system by a local parameter $\alpha(\mathbf{r})=\hbar\Omega/C_6n(\mathbf{r})^2$ and the total Rydberg fraction f_R is given by ($d=3$, $p=6$),

$$f_R = \frac{1}{N}\int dr^3 f_R(\mathbf{r})n(\mathbf{r}) \sim \frac{1}{(-2/\delta+1)^{3/2}}\alpha^{1/\delta}. \tag{4}$$

Here, α is the peak value in the trap center $\alpha=\hbar\Omega/C_6n(\mathbf{0})^2$. Consequently, we find that the critical exponent δ is not modified by the harmonic trapping potential within the local-density approximation and reduces to the value given in the thermodynamic limit.

B. Experimental setup and procedure

A detailed description of the experimental setup can be found in [8,26] and here only a rough outline of the experimental procedure is given. First, we prepare a magnetically trapped cloud of rubidium atoms spin polarized in the $5S_{1/2}$ state. The atomic cloud has a temperature of 3.4 μK and peak densities n_0 close to 10^{20} m^{-3}. This corresponds to phase-space densities below quantum degeneracy to avoid a bimodal density distribution [25] of a Bose-Einstein condensate. To alter the atomic density without changing the size of the cloud, we use a Landau-Zener sweep technique [9] to alter the number of trapped atoms from $N=1.5\times10^7$ to $N=5\times10^5$. In this process, the temperature remains unchanged and, consequently, the physical dimensions of the cloud. With the known harmonic-oscillator potential of the Ioffe-Pritchard-type trap, all parameters of the atomic clouds are known. The excitation to the $43S_{1/2}$ Rydberg state is done with a resonant two-photon transition via the $5P_{3/2}$ state. To avoid population of the intermediate $5P_{3/2}$ state, the light is detuned with respect to this state by $\delta_L=2\pi\times478$ MHz to the blue. The coupling strength Ω of this effective two-level system is altered from $2\pi\times31$ kHz to $2\pi\times154$ kHz by adjusting the laser intensity. The excitation dynamics are investigated by a variation in the excitation time from 100 ns to 20 μs, which is short compared to the excited-state lifetime of 100 μs. After excitation, the Rydberg atoms are field ionized and the emerging ions are detected with the help of a multichannel plate. The resulting strongly blockaded excitation dynamics is determined by the strong repulsive interaction among Rydberg states, which is in our case given by the isotropic van der Waals interaction with $C_6=-1.7\times10^{19}$ a.u. for the $43S$ state.

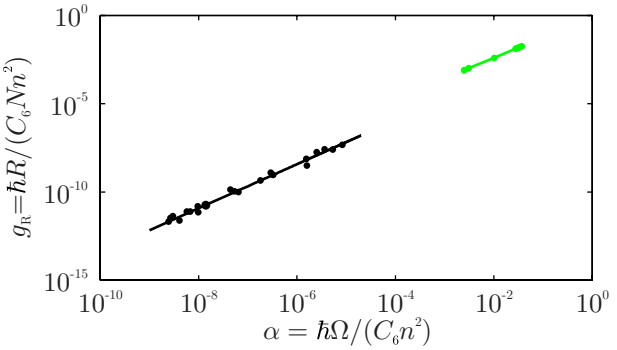

FIG. 3. (Color online) Universal scaling behavior of the excitation rate. The rescaled excitation rate g_R for a three-dimensional density distribution is shown for experimental data (■) and the corresponding numerical simulation (●). A linear fit to a power law $g_R \sim \alpha^\gamma$ results in a critical exponent of $\gamma=1.25\pm0.03$ (expt.) and 1.15 (num).

C. Experimental results

In the experiment, α is changed nonadiabatically by switching on abruptly the coupling laser field Ω. Then, the number of excited Rydberg atoms $N_R(t)$ undergoes a dynamical evolution, which saturates in N_R as shown in Fig. 1(a). The inital increase in the number of Rydberg atoms is well described by a rate R, and this relaxation time is experimentally deduced by a fit of the time evolution of the Rydberg excitation $N_R(t)$ by an exponential saturation function $N_R(t)=N_R(1-e^{-Rt/N_R})$, which allows to extract both the initial excitation rate R and the saturation level N_R. In the strongly blocked regime ($\alpha \ll 1$), the rate R is determined by the collective Rabi frequency $\sqrt{N_b}\Omega$ and the saturation level N_R, which is close to that of the ground state of the system. Previously, we have examined the data and its dependence on the ground-state density n and the Rabi frequency Ω using a general expression $R \sim n^{\kappa_R}\Omega^{\lambda_R}$ and $N_R \sim n^{\kappa_N}\Omega^{\lambda_N}$ [8]. The scaling behavior for a variation in the ground-state density n and the coupling strength Ω gave a strong evidence for a coherent collective excitation dynamics in the strong blockade regime.

In the following, we analyze these results in terms of a universal scaling behavior at resonance ($\Delta=0$) by rescaling the measured quantities to a dimensionless rate g_R and and a dimensionless saturation level f_R as

$$g_R = \frac{\hbar R}{N C_p n^{p/d}} \sim \alpha^\gamma \quad \gamma = \frac{2(p+d)}{2p+d}, \tag{5}$$

$$f_R = \frac{N_R}{N} \sim \alpha^{1/\delta} \quad \delta = \frac{2p+d}{2d}. \tag{6}$$

First, we would like to point out that the data collapse in to algebraic relations, as shown Figs. 1(c) and 3, is in agreement with the predicted scaling laws. It is worth to mention that the numerical simulations based on only 10^2 pseudospins scales up to the experimental situation with atom numbers of up to 10^7. For a more quantitative analysis of the experimental data, it is important to point out that the radial Gaussian radius of the cigar shaped cloud is $\sigma_{x,y}=8.6$ μm.

TABLE I. Comparison of the different results for the critical exponents γ and $1/\delta$ for a three-dimensional (3D) as well a one-dimensional (1D) density distribution. The theoretical values are given in Eqs. (5) and (6). The results of the numerical simulation have been achieved by integrating the Hamiltonian (1) for up to 100 particles [6]. The experimental results are obtained by fitting power laws to the data shown in Figs. 1 and 3.

	γ ($g_R \sim \alpha^\gamma$)	$1/\delta$ ($f_R \sim \alpha^{1/\delta}$)
Experiment (1D)	1.08 ± 0.01	0.16 ± 0.01
Theory	$14/13\approx1.08$	$2/13\approx0.15$
Numerical simulation	1.06	0.150[a]
Experiment (3D)	1.25 ± 0.03	0.45 ± 0.01
Theory	$6/5=1.2$	$2/5=0.4$
Numerical simulation	1.15	0.404[a]

[a]Reference [6].

This width is comparable to the blockade radius between two Rydberg atoms of roughly 5 μm and places by this the geometry in a crossover regime between one and three dimensions. Therefore, we analyze the data whether the experimental setup is better described in one dimension with a line density ($\alpha=\hbar\Omega/C_6n^6$) or in three dimensions ($\alpha=\hbar\Omega/C_6n^2$). Fitting the observed power laws of the form $\ln g_R \sim \gamma \ln \alpha + c_g$ and $\ln f_R \sim 1/\delta \ln \alpha + c_f$, we extracted the individual exponents. The results are summarized in Table I and compared to the expected theoretical values as well as to numerical simulations; the procedure for the numerical analysis is described in detail in [6]. The relatively small error bars of the fitted exponents $1/\delta$ show the excellent agreement with power laws over a large range in α. Nevertheless, the dimensionality cannot unambiguously assigned, although there is a better agreement for the one-dimensional case. Here the exponent is dominated by the variation in density, which scales to the sixth power. In future experiments, it might be possible to create better defined dimensionality by adjusting the shape of the atomic cloud and/or the strength of the interaction by choosing adequate Rydberg states.

IV. DISCUSSION AND OUTLOOK

In summary, we have shown that the experimental results presented in [8] can be described with universal scaling theories. This result confirms that the description with the effective spin Hamiltonian given in this paper is correct to a large extent. Therefore, the observation of a quantum critical point in this system should be within experimental reach. This could be done by measuring the excited Rydberg fraction when approaching the quantum critical point adiabatically starting from a noncritical region in the $\alpha-\Delta$ parameter space. Another way would be the observation of a crystalline correlation function of the excited Rydberg atoms by either a spatial-dependent observation of the Rydberg atoms or in the Fourier space by a Laue diffraction experiment with a four wave mixing technique [27]. The measurement of the critical exponent is not in complete accordance with a one-

dimensional or three-dimensional situation, which is most likely due to finite-size effects. The general form of the scaling exponents allows also to apply the simple model to dipolar systems, which are widely realized in frozen Rydberg gases and are also feasible in the context of ultracold dipolar molecules [28].

ACKNOWLEDGMENTS

We thank the Deutsche Forschunggemeinschaft for financial support within the Grants No. SFB/TRR21 and by No. Pf381/4-1 as well the Landesstiftung Baden Württemberg. B.B. acknowledges support from the Carl Zeiss Stiftung.

[1] K. Huang, *Statistical Mechanics* (John Wiley and Sons, New York, 1987).
[2] G. B. West and J. H. Brown, Phys. Today **57**(9), 36 (2004).
[3] M. H. R. Stanley, L. A. N. Amaral, S. V. Buldyrev, S. Havlin, H. Leschhorn, P. Maass, M. A. Salinger, and H. E. Stanley, Nature (London) **379**, 804 (1996).
[4] M. E. Fisher, Rev. Mod. Phys. **70**, 653 (1998).
[5] M. Greiner, O. Mandel, T. W. Esslinger, T. Hänsch, and I. Bloch, Nature (London) **415**, 39 (2002).
[6] H. Weimer, R. Löw, T. Pfau, and H. P. Büchler, Phys. Rev. Lett. **101**, 250601 (2008).
[7] W. R. Anderson, J. R. Veale, and T. F. Gallagher, Phys. Rev. Lett. **80**, 249 (1998).
[8] R. Heidemann, U. Raitzsch, V. Bendkowsky, B. Butscher, R. Löw, L. Santos, and T. Pfau, Phys. Rev. Lett. **99**, 163601 (2007).
[9] U. Raitzsch, V. Bendkowsky, R. Heidemann, B. Butscher, R. Löw, and T. Pfau, Phys. Rev. Lett. **100**, 013002 (2008).
[10] D. Tong, S. M. Farooqi, J. Stanojevic, S. Krishnan, Y. P. Zhang, R. Côté, E. E. Eyler, and P. L. Gould, Phys. Rev. Lett. **93**, 063001 (2004).
[11] T. Vogt, M. Viteau, J. Zhao, A. Chotia, D. Comparat, and P. Pillet, Phys. Rev. Lett. **97**, 083003 (2006).
[12] A. K. Mohapatra, T. R. Jackson, and C. S. Adams, Phys. Rev. Lett. **98**, 113003 (2007).
[13] T. A. Johnson, E. Urban, T. Henage, L. Isenhower, D. D. Yavuz, T. G. Walker, and M. Saffman, Phys. Rev. Lett. **100**, 113003 (2008).
[14] M. Reetz-Lamour, J. Deiglmayr, T. Amthor, and M. Weidemüller, New J. Phys. **10**, 045026 (2008).
[15] E. Urban, T. A. Johnson, T. Henage, L. Isenhower, D. D. Yavuz, T. G. Walker, and M. Saffman, Nat. Phys. **5**, 110 (2009).
[16] A. Gaëtan, Y. Miroshnychenko, T. Wilk, A. Chotia, M. Viteau, D. Comparat, P. Pillet, A. Browaeys, and P. Grangier, Nat. Phys. **5**, 115 (2009).
[17] K. J. Weatherill, J. D. Pritchard, R. P. Abel, M. G. Bason, A. K. Mohapatra, and C. S. Adams, J. Phys. B **41**, 201002 (2008).
[18] U. Raitzsch, R. Heidemann, H. Weimer, B. Butscher, P. Kollmann, R. Löw, H. P. Büchler, and T. Pfau, New J. Phys. **11**, 055014 (2009).
[19] D. Jaksch, J. I. Cirac, P. Zoller, S. L. Rolston, R. Côté, and M. D. Lukin, Phys. Rev. Lett. **85**, 2208 (2000).
[20] M. D. Lukin, M. Fleischhauer, R. Côté, L. M. Duan, D. Jaksch, J. I. Cirac, and P. Zoller, Phys. Rev. Lett. **87**, 037901 (2001).
[21] E. Brion, K. Mølmer, and M. Saffman, Phys. Rev. Lett. **99**, 260501 (2007).
[22] M. Müller, I. Lesanovsky, H. Weimer, H. P. Büchler, and P. Zoller, Phys. Rev. Lett. **102**, 170502 (2009).
[23] S. Sachdev, *Quantum Phase Transitions* (Cambridge University Press, Cambridge, 1999).
[24] J. V. Hernández and F. Robicheaux, J. Phys. B **41**, 045301 (2008).
[25] R. Heidemann, U. Raitzsch, V. Bendkowsky, B. Butscher, R. Low, and T. Pfau, Phys. Rev. Lett. **100**, 033601 (2008).
[26] R. Löw, U. Raitzsch, R. Heidemann, V. Bendkowsky, B. Butscher, A. Grabowski, and T. Pfau, e-print arXiv:0706.2639.
[27] E. Brekke, J. O. Day, and T. G. Walker, Phys. Rev. A **78**, 063830 (2008).
[28] K.-K. Ni, S. Ospelkaus, M. H. G. de Miranda, A. Pe'er, B. Neyenhuis, J. J. Zirbel, S. Kotochigova, P. S. Julienne, D. S. Jin, and J. Ye, Science **322**, 231 (2008).